

$P_3F_9^{2-}$: An All-Pseudo- π^* 2π -Aromatic

Chakkingal P. Priyakumari[†] and Eluvathingal D. Jemmis^{*,‡}

[†]School of Chemistry, Indian Institute of Science Education and Research Thiruvananthapuram, CET Campus, Thiruvananthapuram, 695 016, Kerala, India

[‡]Department of Inorganic and Physical Chemistry, Indian Institute of Science, Bangalore 560012, India

S Supporting Information

ABSTRACT: A qualitative MO analysis suggests $(PH_3)_3^{2-}$ as a candidate for an all-pseudo- π^* 2π -aromatic; however computational studies rule out its existence. Fluorine substitution which increases the contribution of p orbitals on P in the pseudo- π^* MO makes $(PF_3)_3^{2-}$ a minimum and an aromatic. The 2π aromaticity arising from the bonding combination of the three pseudo- π^* fragment MOs is comparable to that in $C_3O_3^{2-}$ and is another example for the analogy between CO and PF_3 . The dianion $(PF_3)_3^{2-}$ forms the first example of a three-membered ring with all the vertices constituted by pentacoordinate phosphorus. The ability of PF_3 to form the all-pseudo- π^* 2π -aromatic system is not shared by the heavier analogues, AsF_3 and SbF_3 .

Although numerous studies have been done on triangular phosphacycles with tricoordinate phosphorus, corresponding pentacoordinate analogs have not received much attention.¹ There are very few reports on three-membered rings containing pentacoordinate phosphorus;² interestingly, pentacoordinate triphosphirane (**1–4**) is yet to be studied. Schematically triphosphiranes **1**, C_{3h} and **2**, C_s are constructed from trigonal bipyramidal (tbp) PH_5 using one axial and one equatorial bond (Figure 1). Two more structures (**3**, **4**) are obtained starting with an approximate square pyramidal (sqp) PH_5 , the species involved in the turnstile mechanism.³ Here one basal bond is connected to another basal bond of the adjacent P. Our attempt to understand the reason for the absence of any of these structures in literature led to the identification of an all-pseudo-

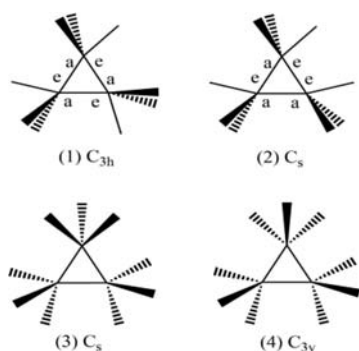


Figure 1. P_3H_9 structures based on tbp (**1**, **2**) and sqp (**3**, **4**).

π^* 2π -aromatic system, $P_3F_9^{2-}$, where aromaticity arises purely from the interaction of pseudo- π^* MOs.

Aromaticity akin to cyclopropenyl cation can arise from a triangular arrangement of three out-of-plane pseudo- π^* levels with the lowest combination having two electrons. Fragments with low pseudo- π^* levels have already been employed to enhance π delocalization, $C_2R_2PF_2^+$ and $C_2R_2SiF_2$ among them.⁴ An interaction diagram involving the Walsh orbitals of hypothetical $(PH_3)_3$ is compared with that of the cyclopropenyl cation in Figure 2. The in-plane p orbitals are involved in the doubly degenerate skeletal MOs, in the cyclopropenyl cation, whereas in $(PH_3)_3$, a mixture of the pseudo- π^* and the pseudo- π orbitals of the PH_3 fragment are involved. The second pseudo- π^* MO of PH_3 with the p orbital perpendicular to the plane forms a standard one-below-two pattern. Only the lower one, LUMO in the neutral structure, is shown. The addition of two electrons must therefore stabilize the structure, generating an ideal 2π aromatic species $(PH_3)_3^{2-}$. The comparable electronegativity values of P and H imply that the pseudo- π^* MO has similar contributions from P and H. The overlap between the pseudo- π^* orbitals will increase if the contributions of the p orbitals on P increases. A way for achieving this is to replace hydrogen atoms by F, as it should result in a larger p orbital contribution on P in the pseudo- π^* fragment MO.

These anticipations were confirmed by computations on $(PH_3)_3$, $(PH_3)_3^{2-}$, and their derivatives.⁵ Geometries were optimized using the double hybrid density functional B2PLYP⁶ and the basis set 6-311++g(d,p). B2PLYP is a general purpose density functional for molecules, which is a major improvement over B3LYP, by adding a perturbative second-order correlation part. Minima on the potential energy surface were located by vibrational frequency analysis at the same level. Calculations were done at the MP2/6-311++g(d,p) level as well, which produced similar results. NICS⁷ values were computed at the GIAO-MP2/6-311++g(d,p) level of theory to gauge the extent of aromaticity.⁸

The structures $(PH_3)_3$ and $(PH_3)_3^{2-}$ could not be obtained as minima. The σ -bonds arising from the pseudo- π^* orbitals do not lend enough stability to $(PF_3)_3$ either. Geometry optimization resulted in the collapse of $(PF_3)_3$ and $(PH_3)_3$ into the corresponding monomers. On the other hand, triangular $(PF_3)_3^{2-}$ (**5**) was obtained as a minimum with C_s symmetry, similar to **3**. Forcing the structure to 3-fold symmetry gave a C_{3h} structure similar to **1**, with three small

Received: August 10, 2013

Published: October 17, 2013

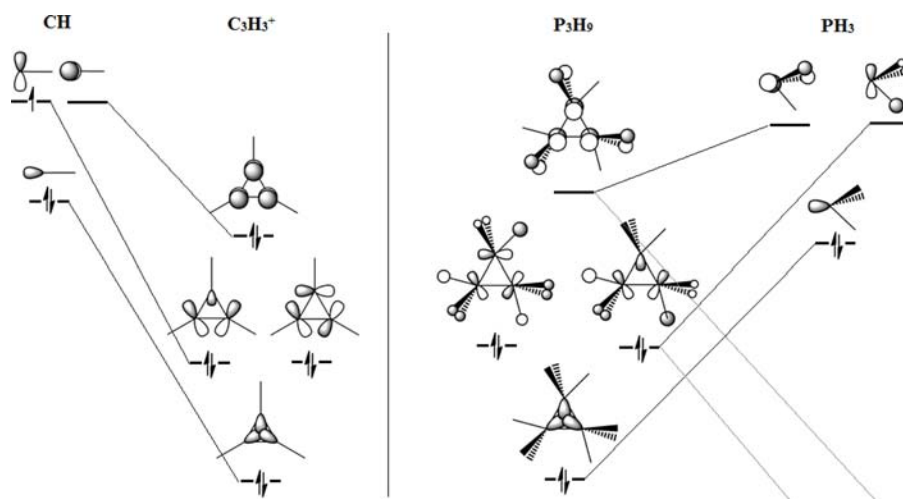


Figure 2. Correlation diagram involving the Walsh orbitals of $C_3H_3^+$ and hypothetical $(PH_3)_3$ (1).

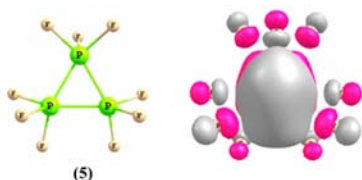


Figure 3. $(PF_3)_3^{2-}$ and the HOMO formed by the overlap of pseudo- π^* orbitals.

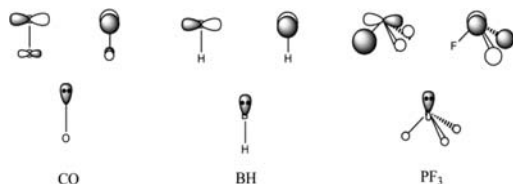


Figure 4. Frontier orbitals of CO, BH, and PF_3 .

Table 1. Comparison of NICS values of $C_3H_3^+$, $B_3H_3^{2-}$, $(PF_3)_3^{2-}$, and $(CO)_3^{2-}$

	NICS(0)	NICS(1)	NICS _{zz} (0)	NICS _{zz} (1)
$C_3H_3^+$	-23.3	-14.9	-30.5	-29.2
$B_3H_3^{2-}$	-16.4	-16.4	-19.1	-27.0
$(PF_3)_3^{2-}$	-38.5	-17.1	-26.7	-16.9
$(CO)_3^{2-}$	-35.2	-7.9	-7.4	-6.5

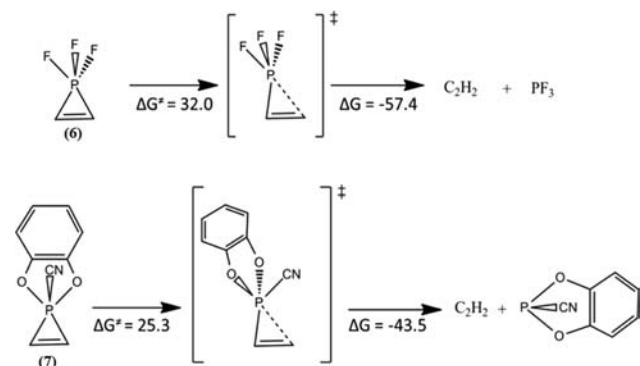


Figure 5. Thermolysis of $C_2H_2PF_3$ and the model system. Energy is in kcal/mol.

imaginary frequencies (-32 , -31 , and -20 cm^{-1}), corresponding to PF_3 rotation, the removal of which led to **5**. The C_{3h} structure is 1.1 kcal/mol higher in energy than the C_s structure (**5**). Similarly a C_{3v} structure similar to **4** and a C_s structure similar to **2** led to **5** on optimization. All three P atoms in the C_s structure **5** have geometries closer to a sqp than to a tbp. On the other hand, the local geometry around P in the C_{3h} stationary point is in between the two, the average deviation from tbp and sqp being very similar. As expected by the symmetry of the C_s structure **5**, one of the P–P bond lengths is shorter (2.207 Å) compared to the other two (2.214 Å). The average P–P bond distance in $(PF_3)_3^{2-}$ is 2.212 Å which is comparable to that in P_4 (2.215 Å). The HOMO, which is formed by the strong in-phase interaction among the out-of-plane pseudo- π^* orbitals of PF_3 fragments, make $(PF_3)_3^{2-}$ a 2π -aromatic system (Figure 3). NICS calculations support this argument with the NICS_{zz}(0) and NICS_{zz}(1) values of -26.7 and -16.9 respectively. The involvement of pseudo- π^* orbitals, which are antibonding along the P–F bond, in the skeletal bonding of $(PF_3)_3^{2-}$ results in an elongation of the P–F bond (1.704 Å) relative to that in PF_3 (1.600 Å).

As the electronegativity difference between P and X (X is a halogen) decreases as X is varied from F to I, the probability for the existence of $(PX_3)_3^{2-}$ also decreases. Although we found minima for other halogens as well, they are less stable as indicated by the presence of a large number of small vibrational frequencies (<100) (Supporting Information). This is in agreement with the already known uniqueness of PF_3 compared to other phosphines.¹⁰

The aromaticity of $(PF_3)_3^{2-}$ can be called pseudo- π^* aromaticity. Although this term is used in chemistry to describe aromaticity where only one of the delocalizing p orbitals belong to the pseudo- π^* variety, $(PF_3)_3^{2-}$ is the first example for a pseudo- π^* 2π -aromatic system, where the aromaticity arises solely from the overlap of pseudo- π^* orbitals. In the pseudoaromatic phosphirenes ($C_2R_2PL_3$) known in literature, the orbitals involved are the pseudo- π^* MO of PL_2L ($L_2 = \text{catecholate}$, $L = -\text{Ph}$ or $-\text{CN}$) fragment and the p orbitals of CH fragments.² Since the electronegativity difference between P and F is the crucial factor here, no atom or group is more effective than F in stabilizing such a trimeric phosphine dianion.

The 2π aromatic nature of $(PF_3)_3^{2-}$ is analogous to $C_3H_3^+$, $B_3H_3^{2-}$, and $C_3O_3^{2-}$. This is not unusual, in view of the isolobal

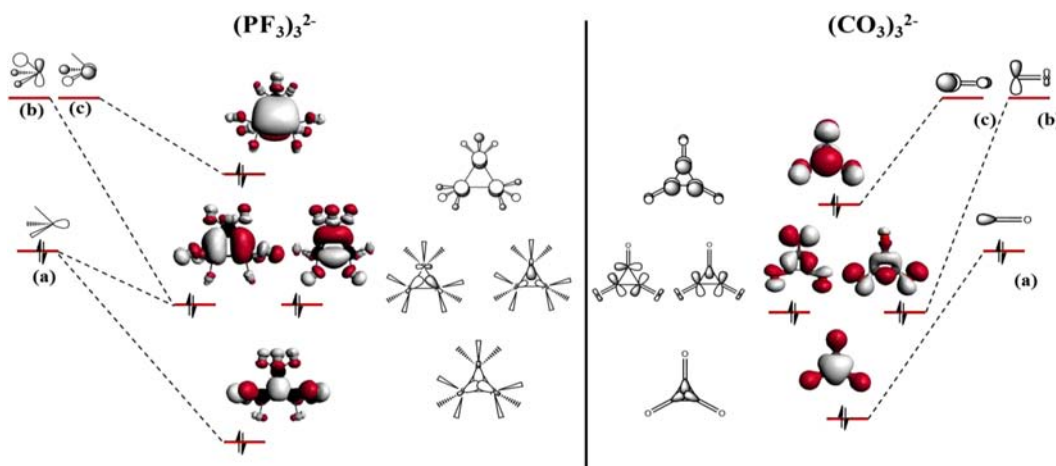
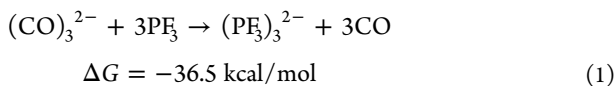


Figure 6. A qualitative FMO diagram of $(\text{PF}_3)_3^{2-}$ and $(\text{CO})_3^{2-}$ at the B3LYP/TZP level.

equivalence of PF_3 to CH^+ , BH , and CO (Figure 4).^{11,12} The HOMO–LUMO gap of $(\text{PF}_3)_3^{2-}$ is 5.6 eV compared to 13.0 eV for C_3H_3^+ and 4.8 eV for $\text{C}_3\text{O}_3^{2-}$, both of which are synthesized.^{11,12} At the MP2/6311++g(d,p) level the gaps are 7.4, 17.2, and 7.3 eV respectively for $(\text{PF}_3)_3^{2-}$, C_3H_3^+ , and $\text{C}_3\text{O}_3^{2-}$.¹³ The in-plane and out-of-plane (1 Å above the ring plane) NICS values and the corresponding zz tensor components of $(\text{PF}_3)_3^{2-}$ are compared to those of C_3H_3^+ , $\text{B}_3\text{H}_3^{2-}$, and $(\text{CO})_3^{2-}$ in Table 1. The values indicate that $(\text{PF}_3)_3^{2-}$ is strongly aromatic, and the aromaticity is higher than that of $\text{C}_3\text{O}_3^{2-}$.

The involvement of the π^* MO of CO in the skeletal bond formation of various CO clusters including $(\text{C}_3\text{O}_3)^{2-}$ was well-studied recently by Borden and co-workers.¹⁴ $(\text{PF}_3)_3^{2-}$ is yet another example of the participation of antibonding fragment MOs in skeletal bond formation, the uniqueness being the pseudo- π^* nature of the fragment MO. The removal of two electrons from $(\text{C}_3\text{O}_3)^{2-}$ to gain neutral C_3O_3 destabilizes the system as indicated by the collapse of C_3O_3 to three CO molecules on optimization.¹⁵ As such one cannot expect a neutral $(\text{PF}_3)_3$ corresponding to pentavalent phosphorus to exist; rather it should exist as a dianion, $(\text{PF}_3)_3^{2-}$.

The NBO analysis indicates a charge of ~ -0.7 on the fluorine atoms of $(\text{PF}_3)_3^{2-}$. Thus counteranions would prefer to coordinate to the fluorine atoms rather than coordinating to the phosphorus atoms. It was found that the geometry and aromaticity of $(\text{PF}_3)_3^{2-}$ are retained in the cation-incorporated system, $(\text{Li}(\text{NH}_3)_2)_2(\text{PF}_3)_3$, as well (Supporting Information). The NICS(0) and NICS(1) of the cation-incorporated $(\text{PF}_3)_3^{2-}$ are -36.0 and -15.8 respectively, which indicates significant aromaticity. The synthesis of deltate anion $\text{C}_3\text{O}_3^{2-}$ from CO via dissolving metal reduction using Na/K alloy in THF/crown ether prompts a similar strategy for $(\text{PF}_3)_3^{2-}$.¹⁶ The relative advantage of PF_3 molecules to form the three-membered ring over CO molecules by capturing electrons can be evaluated by eq 1. The large exothermicity of this reaction indicates a possible synthetic route for $(\text{PF}_3)_3^{2-}$ similar to that of $(\text{CO})_3^{2-}$.



Pentacoordinate phosphorus as part of a three-membered ring is rare. There are very few examples for the structurally characterized pentacoordinate phosphirenes; all of them are

termed as pseudoaromatic as shown by the low reactivity of $\text{C}=\text{C}$.² By isolobally replacing CH^+ of C_3H_3^+ , by PF_3 , one could obtain cyclic $\text{C}_2\text{H}_2\text{PF}_3$ (6). It is reasonable to expect that $\text{C}_2\text{H}_2\text{PF}_3$ might be more stable than any other phosphirene. The energetics of the thermolysis of $\text{C}_2\text{H}_2\text{PF}_3$ relative to a model system analogous to the experimentally known phosphirenes (7) indicates that the former requires higher activation energy for cleavage (Figure 5) indicating greater thermal stability. NICS(1) values for $\text{C}_2\text{H}_2\text{PF}_3$ and the model system of -8.0 and -6.7 , respectively, indicate slightly larger aromaticity for the former. Pentacoordinate P as a part of a four-membered ring is more commonly studied. The pseudorotation of P using the turnstile mechanism is well documented.³

The identification of the possible existence of $(\text{PF}_3)_3^{2-}$ prompted us to look for its heavier analogues. If the electronegativity difference and the consequent large coefficient of pseudo- π^* on the skeletal atom was the only crucial factor, the heavier analogues might form even better clusters. A calculation on the corresponding arsenic cluster, $(\text{AsF}_3)_3^{2-}$, however showed an opposite trend. An approximate C_{3h} symmetric structure was found to be a stationary point on the potential energy surface. This structure has seven small vibrational frequencies ($<100 \text{ cm}^{-1}$) indicating a less stable structure. Moreover, the Wiberg bond index between arsenic atoms is 0.5 indicating a very weak bond. The As–As distance of 2.927 Å is larger than that in As_4 (2.466 Å), indicating weak skeletal bonding. Incorporation of counteranion $\text{Li}(\text{NH}_3)_2^+$ resulted in the rupture of the skeleton. The NICS(0) and NICS(1) values of -20.6 and -14.2 respectively indicate aromaticity as in the case of $(\text{PF}_3)_3^{2-}$. The As–F distance (1.842 Å) has elongated compared to that in AsF_3 (1.752 Å) as expected. The HOMO–LUMO gap is 4.6 eV, lower by 1.0 eV than that of the phosphorus analog. Irrespective of the similar hyperconjugative interaction as in the case of $(\text{PF}_3)_3^{2-}$, the As–As bond is unusually weak in $(\text{AsF}_3)_3^{2-}$. This is understood through a comparison of the fragment analysis, using the ADF program (Figure 6), of $(\text{PF}_3)_3^{2-}$ and $(\text{CO})_3^{2-}$ to $(\text{AsF}_3)_3^{2-}$.¹⁷ The degenerate in-plane skeletal MOs of $(\text{PF}_3)_3^{2-}$ have 60.0% contribution from the radial orbitals, whereas in $(\text{CO})_3^{2-}$ it is only 17.8%. This might weaken the skeletal σ -bonding of $(\text{PF}_3)_3^{2-}$, since the antibonding nature of the degenerate skeletal σ -MOs increases as the contribution from the radial orbital increases. This explains the Wiberg bond index of 1.0 in

(PF₃)₃²⁻ compared to the 1.2 of (CO)₃²⁻. As the σ -framework is too weak to hold the skeleton, occupancy in the π -MO is necessary, which explains why neutral (PF₃)₃ cannot exist. The contribution of the radial orbital to the degenerate σ -MOs increases to 86.8% in (AsF₃)₃²⁻. This increases the antibonding nature of these MOs even further, resulting in a weak As–As bond. The heterosystems P₂AsF₉²⁻ and PAs₂F₉²⁻ are calculated to be minima, but the latter has much lower skeletal bonding indicators. This has been found to be true from the average Wiberg bond index for the skeletal bond which is 0.5 for PAs₂F₉²⁻ and 0.8 for P₂AsF₉²⁻. The weakening of the skeletal bond increases in (SbF₃)₃²⁻ where the WBI index is 0.6 at the B2PLYP/lanl2dzdpp¹⁸ level (at the same level, WBI indices for (AsF₃)₃²⁻ and (PF₃)₃²⁻ are 0.7 and 1.0 respectively).

The analogy between CO and PF₃ has been known since 1950.¹⁰ The π -acceptor ability of PF₃ is comparable to that of CO.¹⁹ This similarity is due to the fact that CO has a low-lying π^* MO that is localized more on C, and PF₃ has a low-lying pseudo- π^* MO that is localized more on P. The deltate anion, (C₃O₃)²⁻, came to the attention of researchers in 1979, whereas its PF₃ analogue remained unnoticed until now.¹² (PF₃)₃²⁻ is the first example for an all-pseudo- π^* 2 π -aromatic system. It should be possible to synthesize (PF₃)₃²⁻ via a procedure similar to the synthesis of C₃O₃²⁻ from CO via dissolving metal reduction.¹⁶ The heavier analogues, (AsF₃)₃²⁻ and (SbF₃)₃²⁻, are more weakly bound and may be harder to realize.

■ ASSOCIATED CONTENT

● Supporting Information

Details of calculations. This material is available free of charge via the Internet at <http://pubs.acs.org>.

■ AUTHOR INFORMATION

Corresponding Author

jemmis@ipc.iisc.ernet.in

Notes

The authors declare no competing financial interest.

■ ACKNOWLEDGMENTS

C.P.K. and E.D.J. thank IISER Thiruvananthapuram and CMSD, University of Hyderabad for providing computational facilities. C.P.K. thanks CSIR-India for research fellowship. DST is acknowledged for the J. C. Bose fellowship to E.D.J.

■ REFERENCES

- (1) Tho Nguyen, M.; Dransfeld, A.; Landuyt, L.; Vanquickenborne, L. G.; Schleyer, P. v. R. *Eur. J. Inorg. Chem.* **2000**, 2000, 103. Tokitoh, N.; Tsurusaki, A.; Sasamori, T. *Phosphorus, Sulphur Silicon Rel. Elem.* **2009**, 184, 979.
- (2) Ehle, M.; Wagner, O.; Bergsträsser, U.; Regitz, M. *Tetrahedron Lett.* **1990**, 31, 3429. Sase, S.; Kano, N.; Kawashima, T. *J. Am. Chem. Soc.* **2002**, 124, 9706. Sase, S.; Kano, N.; Kawashima, T. *J. Org. Chem.* **2006**, 71, 5448.
- (3) Hoffmann, R.; Howell, J. M.; Muetterties, E. L. *J. Am. Chem. Soc.* **1972**, 94, 3047. Clennan, E. L.; Heah, P. C. *J. Org. Chem.* **1983**, 48, 2621.
- (4) Göller, A.; Heydt, H.; Clark, T. *J. Org. Chem.* **1996**, 61, S840. Göller, A.; Clark, T. *J. Mol. Model.* **2000**, 6, 133.
- (5) Frisch, M. J., et al. *Gaussian 09*, revision A.02; Gaussian, Inc.: Wallingford, CT, 2009.
- (6) Grimme, S. *J. Chem. Phys.* **2006**, 124, 034108.
- (7) Schleyer, P. v. R.; Maerker, C.; Dransfeld, A.; Jiao, H.; Hommes, N. J. R. v. E. *J. Am. Chem. Soc.* **1996**, 118, 6317.

(8) Head-Gordon, M.; Pople, J. A.; Frisch, M. J. *J. Chem. Phys. Lett.* **1988**, 153, 503.

(9) Mealli, C.; Proserpio, D. M. *J. Chem. Educ.* **1990**, 67, 399. Hoffmann, R. *J. Chem. Phys.* **1963**, 39, 1397. Hoffmann, R.; Lipscomb, W. N. *J. Chem. Phys.* **1962**, 36, 2179.

(10) Chatt, J. *Nature* **1950**, 165, 637.

(11) Breslow, R.; Groves, J. T. *J. Am. Chem. Soc.* **1970**, 92, 984. Lednor, P. W.; Versloot, P. C. *J. Chem. Soc., Chem. Commun.* **1983**, 284. Wehrmann, R.; Meyer, H.; Berndt, A. *Angew. Chem., Int. Ed. Engl.* **1985**, 24, 788. Eisch, J. J.; Shafii, B.; Odom, J. D.; Rheingold, A. L. *J. Am. Chem. Soc.* **1990**, 112, 1847. Jemmis, E. D.; Subramanian, G.; Srinivas, G. N. *J. Am. Chem. Soc.* **1992**, 114, 7939. Seitz, G.; Imming, P. *Chem. Rev.* **1992**, 92, 1227. Krempp, M.; Damrauer, R.; DePuy, C. H.; Keheyuan, Y. *J. Am. Chem. Soc.* **1994**, 116, 3629. Korkin, A. A.; Schleyer, P. v. R.; McKee, M. L. *Inorg. Chem.* **1995**, 34, 961.

(12) West, R.; Eggerding, D.; Perkins, J.; Handy, D.; Tuazon, E. C. *J. Am. Chem. Soc.* **1979**, 101, 1710.

(13) Pearson, R. G. *J. Org. Chem.* **1989**, 54, 1423. Zhou, Z.; Parr, R. G. *J. Am. Chem. Soc.* **1989**, 111, 7371. Zhou, Z.; Parr, R. G. *J. Am. Chem. Soc.* **1990**, 112, 5720.

(14) Bao, X.; Zhou, X.; Lovitt, C. F.; Venkatraman, A.; Hrovat, D. A.; Gleiter, R.; Hoffmann, R.; Borden, W. T. *J. Am. Chem. Soc.* **2012**, 134, 10259.

(15) Schleyer, P. v. R.; Najafian, K.; Kiran, B.; Jiao, H. *J. Org. Chem.* **2000**, 65, 426.

(16) Mathre, D. J.; Guida, W. C. *Tetrahedron Lett.* **1980**, 21, 4773.

(17) *Scientific Computing & Modeling. ADF*; Vrije Universiteit, Theoretical Chemistry: Amsterdam, The Netherlands, 2012. Te Velde, G.; Bickelhaupt, F. M.; Baerends, E. J.; Guerra, C. F.; Van Gisbergen, S. J. A.; Snijders, J. G.; Ziegler, T. *J. Comput. Chem.* **2001**, 22, 931.

(18) Feller, D. *J. Comput. Chem.* **1996**, 17 (13), 1571. Schuchardt, K. L.; Didier, B. T.; Elsethagen, T.; Sun, L. G. V.; Chase, J.; Li, J.; Windus, T. L. *J. Chem. Inf. Model.* **2007**, 47 (3), 1045.

(19) Green, J. C.; King, D. I.; Eland, J. H. D. *J. Chem. Soc. D* **1970**, 1121. Head, R. A.; Nixon, J. F.; Sharp, G. J.; Clark, R. J. *J. Chem. Soc., Dalton Trans.* **1975**, 2054. Corderman, R. R.; Beauchamp, J. L. *Inorg. Chem.* **1977**, 16, 3135. Balch, A. L.; Davis, B. J.; Olmstead, M. M. *J. Am. Chem. Soc.* **1990**, 112, 8592. Braga, M. *THEOCHEM* **1992**, 253, 167. Ehlers, A. W.; Baerends, E. J.; Bickelhaupt, F. M.; Radius, U. *Chem.—Eur. J.* **1998**, 4, 210. Bickelhaupt, F. M.; Radius, U.; Ehlers, A. W.; Hoffmann, R.; Baerends, E. J. *New J. Chem.* **1998**, 22, 1. Radius, U.; Bickelhaupt, F. M.; Ehlers, A. W.; Goldberg, N.; Hoffmann, R. *Inorg. Chem.* **1998**, 37, 1080. Seuret, P.; Weber, J.; Wesolowski, T. A. *Mol. Phys.* **2003**, 101, 2537. Yang, H.-Q.; Li, Q.-S.; Xie, Y.; King, R. B.; Schaefer, H. F. *Mol. Phys.* **2010**, 108, 2477. Yang, H.-q.; Li, Q.-s.; Xie, Y.; King, R. B.; Schaefer, H. F. *J. Phys. Chem. A* **2010**, 114, 8896.